Detailed Simplified Implementation of Filter Bank Multicarrier Modulation Using Sub-Channel Prototype Filters

Mohammad M. Banat and Ahmed A. Al-Shwmi

banat@just.edu.jo, engalshomi@hotmail.com

Department of Electrical Engineering, Jordan University of Science and Technology

Abstract: -Filter bank multicarrier modulation is one of the most researched techniques in recent wireless communications literature. It is robust against channel frequency selectivity, but it does not require cyclic prefix to compensate for intersymbol interference. Therefore, filter bank multicarrier modulation is superior to orthogonal frequency division multiplexing in terms of spectral efficiency. However, this comes at the cost of higher implementation complexity.

Despite the vast published research on filter bank multicarrier modulation, little attention has been given to providing a detailed implementation supported by sufficient mathematical analysis. This is particularly true about the prototype filter section, which is the main source of implementation complexity. In this paper we try to fill this gap by presenting a detailed implementation based on the use of simple sub-channel prototype filters. Sub-channel prototype filters are shorter than a single prototype filter by a factor that is equal to the number of data symbols per multicarrier symbol, resulting in reduced complexity and added design flexibility. Detailed mathematical analysis is provided to support the validity of the proposed implementation.

Keywords: multicarrier modulation, filter banks, orthogonal frequency division multiplexing.

I. Introduction

Future wireless systems should support a large range of possible use cases, such as high data rate services, point to-point or point to multipoint communication and low-latency transmissions. This requires efficient utilization of the available time/frequency resources. In orthogonal frequency division multiplexing (OFDM), this is difficult to achieve; due to its weak spectral efficiency due to insert cyclic prefix.

A multicarrier modulation (MCM) signal consists of the superposition of a number of sinusoidal subcarriers [1], a process through which the total signal bandwidth is divided into many narrowband sub-channel signals to be transmitted simultaneously. In other words, an MCM signal is the result of splitting up a wideband signal having a high symbol rate into several lower rate signals, each one having a lower symbol rate and occupying a narrower bandwidth [2].

MCM signals are known to be robust to multipath fading [2]. This is why MCM signals are usually used when transmission is performed over frequency selective fading channels. The bandwidths of MCM sub-channels are chosen so that they are lower than the coherence bandwidth of the communication channel. Therefore, even though the overall communication channel may be frequency selective, the sub-channels can be made frequency flat.

Recently, MCM has become very attentive in wireless communications, specifically for multimedia transmission. This is mainly due to the ever increasing human need for transmitting signals at higher data rates. Applications involving multimedia signals are top candidates in this regard. Needless to say, next generation (and beyond) wireless communication systems place great emphasis on applications involving high data rate multimedia signals [3]. There are various types of MCM, and some of them have already been used in some applications, including spatial modulation (SM) and orthogonal frequency division multiplexing with index modulation (IM) [4].

Filter bank multicarrier (FBMC) modulation is an alternative to OFDM that has better spectral properties [5]. Contrary to OFDM, FBMC does not need the so-called cyclic prefix (CP) to avoid intersymbol interference (ISI). The new concepts of dynamic access spectrum management (DASM) and cognitive radio require high resolution spectral analysis, a functionality in which filter banks are superior to the discrete Fourier transform of OFDM [6]. FBMC requires higher implementation complexity than OFDM.

The main contribution of this paper is the development of a detailed simplified implementation of the FBMC modulator and demodulator with sub-channel prototype filters. Sub-channel prototype filters are shorter than a single prototype filter by a factor that is equal to the number of data symbols per multicarrier symbol, resulting in reduced complexity and added design flexibility.

The rest of this paper is organized as follows. In section II, we describe the pre-processing stage of FBMC. In section III, we present the inverse discrete Fourier transform (IDFT) stage. In section IV, we present the filtering stage and derive the signal to be transmitted. The reception stage is described in Section V. Conclusions are presented is Section VI.

II. FBMC Pre-Processing

Consider a block of $M = 2Q$ serial (generally complex-valued) quadrature amplitude modulation (QAM) symbols $x_{m,n}\Big|_{m=0}^{M-1}$, where n represents discrete time index of the block of symbols. Letting each QAM symbol have a duration T_s, the duration of the whole symbol block is then equal to

$$T = MT_s \tag{1}$$

The QAM symbols can be decomposed into real and imaginary parts by using complex to real conversion as follow:

$$x_{m,n} = x_{m,n}^R + jx_{m,n}^I \tag{2}$$

where

$$\begin{aligned} x_{m,n}^R &= \mathrm{Re}\{x_{m,n}\} \\ x_{m,n}^I &= \mathrm{Im}\{x_{m,n}\} \end{aligned} \tag{3}$$

Let

$$\begin{aligned} \tau &= \frac{T}{2} \\ &= QT_s \end{aligned} \tag{4}$$

The continuous-time multicarrier signal at the output of the modulator is given by [2]

$$v(t) = \sum_{l=-\infty}^{\infty} \sum_{q=0}^{Q-1} \left(\begin{aligned} & v_{2q,l}(t) e^{j2\pi(2q)\Delta f t} \\ & + v_{2q+1,l}(t) e^{j2\pi(2q+1)\Delta f t} \end{aligned} \right) \tag{5}$$

where

$$v_{2q,l}(t) = \left. \begin{aligned} & x_{2q,l}^R z(t - 2l\tau) \\ & + jx_{2q,l}^I z\big(t - (2l+1)\tau\big) \end{aligned} \right|_{q=0}^{Q-1} \tag{6}$$

$$v_{2q+1,l}(t) = \left. \begin{aligned} & jx_{2q+1,l}^I z(t - 2l\tau) \\ & + x_{2q+1,l}^R z\big(t - (2l+1)\tau\big) \end{aligned} \right|_{q=0}^{Q-1} \tag{7}$$

where $z(t)$ is an even real-valued pulse shape that generally extends for $-\infty < t < \infty$, and Δf is the subcarrier spacing, given by

$$\Delta f = \frac{1}{T} \tag{8}$$

Note that Δf is equal to the reciprocal of the multicarrier symbol period T. Let

$$\begin{aligned} d_{2q,2l} &= x_{2q,l}^R \\ d_{2q,2l+1} &= jx_{2q,l}^I \end{aligned} \tag{9}$$

$$\begin{aligned} d_{2q+1,2l} &= jx_{2q+1,l}^I \\ d_{2q+1,2l+1} &= x_{2q+1,l}^R \end{aligned} \tag{10}$$

The operation performed in (9) is the first part of the pre-processing (staggering) stage, and is represented as in Figure 1.

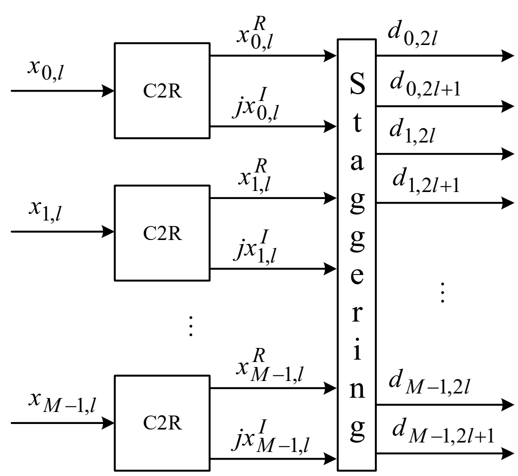

Figure 1: First part of pre-processing operation

Substituting (9) into (6) and (7) yields

$$\begin{aligned} v_{2q,l}(t) &= d_{2q,2l} z(t - 2l\tau) \\ &+ d_{2q,2l+1} z\big(t - (2l+1)\tau\big) \end{aligned} \tag{11}$$

$$\begin{aligned} v_{2q+1,l}(t) &= d_{2q+1,2l} z(t - 2l\tau) \\ &+ d_{2q+1,2l+1} z\big(t - (2l+1)\tau\big) \end{aligned} \tag{12}$$

Let $m = 2q$ in (11) and $m = 2q+1$ in (12) to get

$$v_{m,l}(t) = \left. \begin{array}{l} d_{m,2l} z(t-2l\tau) \\ +d_{m,2l} z\left(t-(2l+1)\tau\right) \end{array} \right|_{m=0}^{M-1} \quad (13)$$

The last result allows (5) to be rewritten in the form

$$v(t) = \sum_{l=-\infty}^{\infty} \sum_{m=0}^{M-1} v_{m,l}(t) e^{j2\pi m\Delta ft} \quad (14)$$

Similar steps to the above can be performed on the index l in (13), so that (5) simplifies to

$$v(t) = \sum_{n=-\infty}^{\infty} \sum_{m=0}^{M-1} d_{m,n} z(t-n\tau) e^{j2\pi m\Delta ft} \quad (15)$$

The sequence $d_{m,n}$ in (15) is obtained from the outputs of Figure 1 through the second part of the pre-processing stage, as shown in Figure 2.

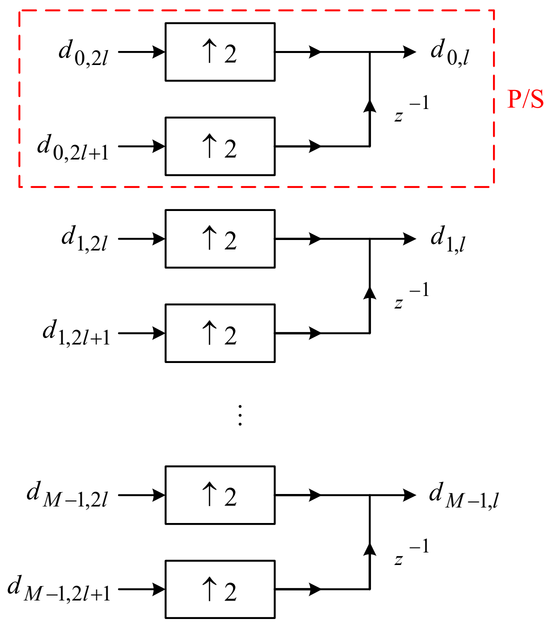

Figure 2: Second part of pre-processing operation

III. IDFT Stage

The pulse shaping waveform $z(t)$ is obviously uncausal. Let $z(t)$ be negligibly small for $|t| > (L-1)T_s/2$, for some odd integer L, that is chosen such that

$$L = 2\Gamma + 1 \quad (16)$$

where $\Gamma = FM$ and F is an integer number. Note that with the last assumption on L, $z(t)$ is negligibly small for $|t| > \Gamma T_s$. Let $z_{tr}(t)$ be a truncated version of $z(t)$, such that

$$z_{tr}(t) = \begin{cases} z(t), & |t| \le \Gamma T_s \\ 0, & \text{otherwise} \end{cases} \quad (17)$$

Let's define the causal waveform $z_c(t)$, extending for $0 \le t \le 2\Gamma T_s$, as follows

$$z_c(t) = z_{tr}(t - \Gamma T_s) \quad (18)$$

Without loss of generality, and to simply signal expressions that will be obtained later, we let

$$z_c(2\Gamma T_s) = 0 \quad (19)$$

Let $z_c(t)$ be sampled every T_s, for all $0 \le k \le 2\Gamma$, to produce the sequence $p[k]$, according to

$$p[k] = z_c(kT_s) \quad (20)$$

Then we have

$$p[k] = z_{tr}((k-\Gamma)T_s) \quad (21)$$

From (19),

$$p[2\Gamma] = 0 \quad (22)$$

To create a causal discrete-time transmitted sequence, let

$$s[k] = v((k-\Gamma)T_s) \quad (23)$$

Using $z_{tr}(t)$ in place of $z(t)$ and substituting (21), (1) and (8) in (23) yields

$$s[k] = \sum_{n=-\infty}^{\infty} \sum_{m=0}^{M-1} d_{m,n} p[k-nQ] e^{j\frac{2\pi}{M}mk} \quad (24)$$

Note that $p[k-nQ]$ in (24) is non-zero only when

$$0 \le k - nQ < 2\Gamma \quad (25)$$

This can be rearranged into the form

$$\frac{k}{Q} - 4F < n \le \frac{k}{Q} \quad (26)$$

Let the high rate time index k be decomposed in terms of a lower rate time index l as follows

$$k = lQ + q \quad (27)$$

where $q = 0, \cdots, Q-1$. Then,

$$l - 4F + \frac{q}{Q} < n \le l + \frac{q}{Q} \quad (28)$$

Since n is an integer and $0 \le q \le Q-1$, the lowest possible value of n is $l - 4F + 1$ and the largest value of n is l. Hence, we can rewrite (24) in the form

$$s_{q,l} = \sum_{n=l-4F+1}^{l} p_{q,l-n} \sum_{m=0}^{M-1} d_{m,n} e^{j\frac{2\pi}{M}m(lQ+q)} \quad (29)$$

where

$$s_{q,l} = s[lQ + q] \tag{30}$$

$$p_{q,n} = p[nQ + q] \tag{31}$$

Changing variables in the outer summation in (29), we get

$$s_{q,l} = \sum_{n=0}^{4F-1} p_{q,n} \sum_{m=0}^{M-1} d_{m,l-n} e^{j\frac{2\pi}{M}m(lQ+q)} \tag{32}$$

Simple manipulation of (32) yields

$$\begin{aligned} s_{q,l} &= \sum_{n=0}^{4F-1} p^e_{q,n} \sum_{m=0}^{Q-1} d_{2m,l-n} e^{j\frac{2\pi}{Q}mq} \\ &+ \sum_{n=0}^{4F-1} p^o_{q,n} \sum_{m=0}^{Q-1} d_{2m+1,l-n} e^{j\pi(l-n)} e^{j\frac{2\pi}{Q}mq} \end{aligned} \tag{33}$$

where

$$p^e_{q,n} = p_{q,n} \tag{34}$$

$$p^o_{q,n} = p_{q,n} e^{j\frac{2\pi}{M}(nQ+q)} \tag{35}$$

Let

$$\begin{aligned} a^e_{q,l} &= \sum_{m=0}^{Q-1} d_{2m,l} e^{j\frac{2\pi}{Q}mq} \\ &= \mathrm{IFFT}\left\{ d_{2m,l}\Big|_{m=0}^{Q-1} \right\} \end{aligned} \tag{36}$$

The IDFT operation in (36) is illustrated as in Figure 3.

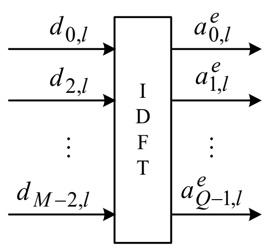

Figure 3: Even IDFT

$$\begin{aligned} a^o_{q,l} &= \sum_{m=0}^{Q-1} d_{2m+1,l} e^{j\pi l} e^{j\frac{2\pi}{Q}mq} \\ &= \mathrm{IFFT}\left\{ d_{2m+1,l} e^{j\pi l}\Big|_{m=0}^{Q-1} \right\} \end{aligned} \tag{37}$$

The IDFT operation in (37) is illustrated as in Figure 4.

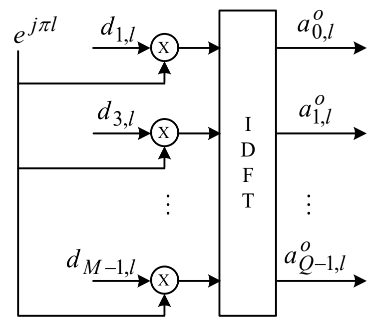

Figure 4: Odd IDFT

IV. Filtering Stage and Transmitted Signal

Equation (33) can be rewritten in the form

$$s_{q,l} = \sum_{n=0}^{4F-1} p^e_{q,n} a^e_{q,l-n} + \sum_{n=0}^{4F-1} p^o_{q,n} a^o_{q,l-n} \tag{38}$$

Equivalently, we have

$$s_{q,l} = p^e_{q,l} * a^e_{q,l} + p^o_{q,l} * a^o_{q,l} \tag{39}$$

The filtering of the even and odd IDFT sequences, that is performed in (39) is represented as in Figure 5.

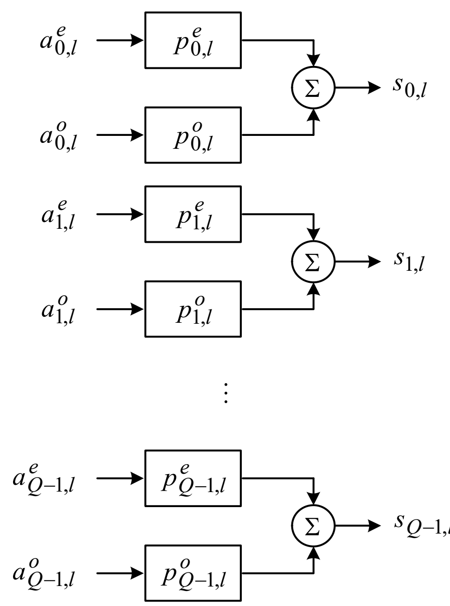

Figure 5: Filtering of IDFT outputs

A parallel-to-serial operation is used to sequentially arrange the filtered IDFT outputs, as shown in Figure 6.

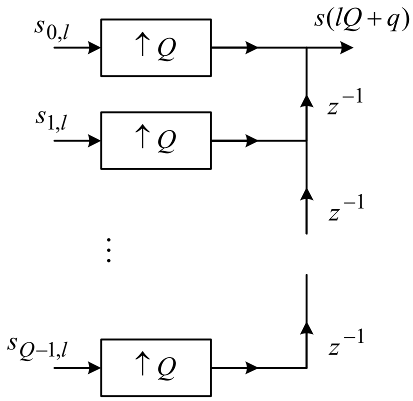

Figure 6: Parallel-to-serial conversion

As can be seen from (39), and compared to OFDM, the size-M IDFT operation is replaced by two size-Q IDFT operations, followed by convolutions with sequences of length $4F$ at each IDFT output.

V. Reception

The first step in the reception process it to convert the sequence $s(lQ+q)$ from serial to parallel form. This is illustrated in Figure 7.

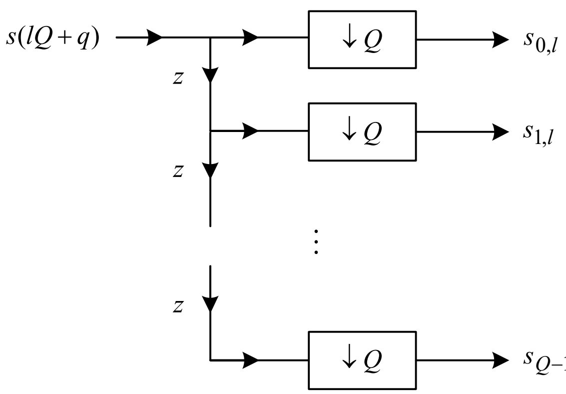

Figure 7: Serial-to-parallel conversion

Note that $d_{m,n}$ can be rewritten in the form

$$d_{m,n} = b_{m,n} e^{j\phi_{m,n}} \tag{40}$$

where

$$\begin{aligned} b_{2q,2l} &= x^R_{2q,l} \\ b_{2q,2l+1} &= x^I_{2q,l} \end{aligned} \tag{41}$$

$$\begin{aligned} b_{2q+1,2l} &= x^I_{2q+1,l} \\ b_{2q+1,2l+1} &= x^R_{2q+1,l} \end{aligned} \tag{42}$$

and

$$\phi_{m,n} = \frac{\pi}{2}(m+n)_2 \tag{43}$$

Letting

$$\gamma_{m,n}[k] = p[k-nQ] e^{j\phi_{m,n}} e^{j\frac{2\pi}{M}mk} \tag{44}$$

Equation (24) can be rewritten in the form

$$s[k] = \sum_{n=-\infty}^{\infty} \sum_{m=0}^{M-1} b_{m,n} \gamma_{m,n}[k] \tag{45}$$

Reception of transmitted symbols can be achieved by generating the sequence

$$\hat{b}_{r,u} = \mathrm{Re}\left\{\tilde{b}_{r,u}\right\} \tag{46}$$

where

$$\tilde{b}_{r,u} = \sum_{k=-\infty}^{\infty} s[k] \gamma^*_{r,u}[k] \tag{47}$$

Substituting (44) into (47) yields

$$\begin{aligned} \tilde{b}_{r,u} &= \sum_{k=-\infty}^{\infty} s[k] p[k-uQ] e^{-j\phi_{r,u}} e^{-j\frac{2\pi}{M}rk} \\ &= \sum_{l=-\infty}^{\infty} e^{-j\phi_{r,u}} e^{-j\pi rl} \\ &\quad \times \sum_{q=0}^{Q-1} s_{q,l} p_{q,l-u} e^{-j\frac{2\pi}{M}rq} \end{aligned} \tag{48}$$

Note that $p_{q,l-u}$ is non-zero in the range

$$u \le l < 4F + u \tag{49}$$

This allows (48) to be written as

$$\begin{aligned} \tilde{b}_{r,u} &= \sum_{l=u}^{4F-1+u} e^{-j\phi_{r,u}} e^{-j\pi rl} \\ &\quad \times \sum_{q=0}^{Q-1} s_{q,l} p_{q,l-u} e^{-j\frac{2\pi}{M}rq} \end{aligned} \tag{50}$$

By a change of variables, (50) becomes

$$\begin{aligned} \tilde{b}_{r,u} &= \sum_{l=0}^{4F-1} e^{-j\phi_{r,u}} e^{-j\pi rl} \\ &\quad \times \sum_{q=0}^{Q-1} s_{q,l+u} p_{q,l} e^{-j\frac{2\pi}{M}rq} \end{aligned} \tag{51}$$

For even $r = 2i$,

$$\tilde{b}_{2i,u} = e^{-j\phi_{2i,u}} \sum_{q=0}^{Q-1} g_{q,u}^{e} e^{-j\frac{2\pi}{Q}iq} \tag{52}$$

where

$$\begin{aligned} g_{q,u}^{e} &= \sum_{l=0}^{4F-1} s_{q,l+u}\, p_{q,l}^{e} \\ &= s_{q,l} * p_{q,-l}^{e} \end{aligned} \tag{53}$$

Based on the last result,

$$\tilde{b}_{2i,u} = e^{-j\phi_{2i,u}}\, \mathrm{DFT}\left\{ g_{q,u}^{e} \Big|_{q=0}^{Q-1} \right\} \tag{54}$$

For odd $r = 2i+1$,

$$\tilde{b}_{2i+1,u} = e^{-j\phi_{2i+1,u}} \sum_{q=0}^{Q-1} g_{q,u}^{o} e^{-j\frac{2\pi}{M}iq} \tag{55}$$

$$\begin{aligned} g_{q,u}^{o} &= \sum_{l=0}^{4F-1} s_{q,l+u}\, p_{q,l}^{o*} \\ &= s_{q,l} * p_{q,-l}^{o*} \end{aligned} \tag{56}$$

Based on the last result,

$$\tilde{b}_{2i+1,u} = e^{-j\phi_{2i+1,u}}\, \mathrm{DFT}\left\{ g_{q,u}^{o} \Big|_{q=0}^{Q-1} \right\} \tag{57}$$

The first step in the receiver is, therefore, to generate the sequences $g_{q,u}^{e}$ and $g_{q,u}^{o}$. This is done using (53) and (56), and is illustrated in Figure 8.

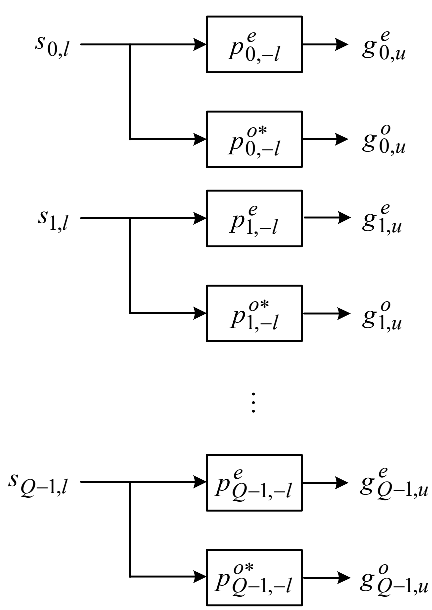

Figure 8: Filtering of DFT inputs

Generation of even- and odd-numbered samples of the sequence $\tilde{b}_{r,u}$ is illustrated in Figure 9 and Figure 10.

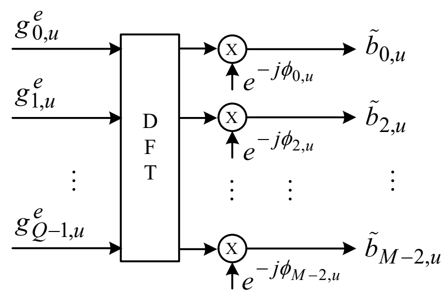

Figure 9: Even DFT

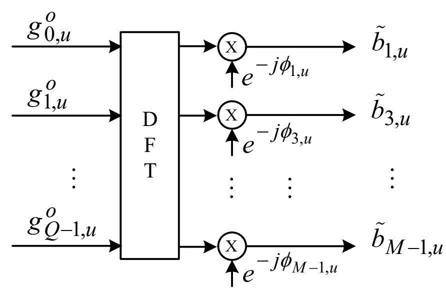

Figure 10: Odd DFT

VI. Conclusion

The paper has presented a detailed simplified implementation of a filter bank multicarrier transmitter and receiver with sub-channel prototype filters. Sub-channel prototype filters are shorter than a single prototype filter by a factor that is equal to the number of data symbols per multicarrier symbol, resulting in reduced complexity and added design flexibility. Exploitation of the flexibility resulting from the use of sub-channel prototype filters is to be considered in future research.

References

[1] J. A. C. Bingham, "Multicarrier modulation for data transmission: An idea whose time has come," *IEEE Communications Magazine,* vol. 28, no. 5, pp. 5-14, May 1990.

[2] P. Siohan, C. Siclet and N. Lacaille, "Analysis and Design of OFDM/OQAM Systems Based on Filterbank Theory," *IEEE Transactions on Signal Processing,* vol. 50, no. 5, pp. 1170-1183, May 2002.

[3] D. Bethanabhotla, G. Caire and M. J. Neely, "WiFlix: Adaptive Video Streaming in

Massive MU-MIMO Wireless Networks," *IEEE Transactions on Wireless Communications,* vol. 15, no. 6, pp. 4088-4103, Jun. 2016.

[4] E. Basar, "Index modulation techniques for 5G wireless networks," *IEEE Communications Magazine,* vol. 54, no. 7, pp. 168-175, July 2016.

[5] B. Farhang-Boroujeny, "Filter bank multicarrier modulation: A waveform candidate for 5G and beyond," *Advances in Electrical Engineering,* 2014.

[6] B. Farhang-Boroujeny and R. Kempter, "Multicarrier communication techniques for spectrum sensing and communication in cognitive radios," *IEEE Communications Magazine,* vol. 46, no. 4, pp. 80-85, Apr. 2008.